Signal Amplification by Magnetic Force on Polydiacetylene Supramolecules for Detection of Prostate Cancer

*Il Kyoung Kwon, Min Sun Song, Sang Ho Won, Seung Phill Choi, Moonil Kim, and Sang Jun Sim**

Medical diagnostic sensor technology depends on enhancement of the sensitivity and selectivity of sensor materials. Conjugated polymers (CPs) are important materials that have recently received considerable attention. In particular, polydiacetylene (PDA) represents one of the most intensively researched conjugated polymers and has been demonstrated to have very effective sensing properties.[1–3] Closely packed diacetylene lipids such as 10,12-pentacosadiynoic acid (PCDA) can undergo polymerization via a 1,4-addition reaction upon UV irradiation, forming ene-yne alternating polymer chains without additional catalysts or initiators. Polymerized PCDA exposed to 254 nm UV light generally undergoes a color change from blue to red in response to various stimuli, including heat, organic solvents, mechanical force, pH, and ligand–receptor interactions that occur at the PDA matrix interface.[4,5–9] Moreover, PDA vesicles generate fluorescence in their red state, which enhances their applicability in terms of elucidating their optical signals. Based on these unique properties, PDA-based sensors have been developed to detect biological specimens, viruses, DNA, *Escherichia coli* (*E. coli*), glucose, cyclodextrin, and proteins.[10–12]

Prostate-specific antigen (PSA) has been established as a valuable biomarker for the diagnosis of prostate cancer.[13] PSA in human serum is either free or in complex with two major proteinase inhibitors, α_1-antichymotrysin (PSA-ACT, molecular weight, MW, 90 kDa) and α_2-macroglobulin (PSA-AMG). The molecular size and weight of the analytes greatly affect the fluorescence of PDA vesicles.[14,15] Changes in fluorescence in the case of the PSA-ACT complex are relatively low since proteins, which are much smaller compared to bacteria or viruses, are insufficient in size to press the PDA vesicles, whereas larger biomolecules sharply change the fluorescence.[16]

Recently, biosensors have been developed using magnetic beads for the purpose of increasing the sensitivity of target detection.[17,18] Based on this, many researchers are currently investigating applications to enhance the sensitivity and specificity via active guiding of magnetic beads using sensor-generated magnetic forces. Here, we introduce a novel method based on PDA vesicles for enhanced detection. This strategy involves amplification of the fluorescent signal by combining the primary immune reaction of the antigen-antibody, the sandwich method of the pAb-conjugated magnetic beads, and amplification of the fluorescent signal due to mechanical pressure caused by a permanent magnet.

We describe a strategy for the detection of the PSA-ACT complex using solid PDA vesicle chips based on amplification of fluorescence by PSA pAb-conjugated magnetic beads. Moreover, as shown in **Scheme 1**, an "attraction method" in which a permanent magnet was introduced onto the PDA vesicles chips is introduced for further enhancement of the fluorescence of PDA vesicles. Lastly, the response of the PDA vesicle spots was monitored after introduction of the PSA-ACT complex at various concentrations (0.01 ng mL^{-1} to 10 μg mL^{-1}).

To study the effects of the size of streptavidin (SA)-conjugated magnetic beads on PDA fluorescence, two different sizes of SA-conjugated magnetic beads (100 nm and 1 μm) along with SA were prepared with biotin-conjugated PDA vesicles. The non-fluorescent PDA vesicles were converted into the fluorescent PDA when the SA-conjugated magnetic beads (100 ng mL^{-1}) and SA (100 ng mL^{-1}) were bound to the biotin-PDA. We analyzed changes in fluorescence upon addition of SA-conjugated magnetic beads and SA.

To explain the role of mechanical force in greater detail, electron microscopy was used to probe the morphology of the PDA vesicles bound to the substrates. **Figure 1**a shows scanning electron microscopy (SEM) images of the PDA vesicles immobilized to both SA alone and the SA-conjugated magnetic beads (100 nm and 1 μm). This increase in aggregation indicates that the mechanical force was dramatically greater on the surface of the PDA vesicles, resulting in amplification of the fluorescence signal.

Figure 1B shows the fluorescent responses of the chip and the fluorescent spot images depending on magnetic

I. K. Kwon, Dr. S. P. Choi, Prof. S. J. Sim
Nanobiotechnology Laboratory
Department of Chemical and Biological Engineering
Korea University, Seoul, 136-713, Korea
E-mail: simsj@korea.ac.kr
M. S. Song, S. H. Won
School of Chemical Engineering
Sungkyunkwan University
Suwon, 440-746, Korea
Prof. M. I. Kim
Department of Electrical Engineering
Korea University
Seoul, 136-713, Korea

DOI: 10.1002/smll.201101322

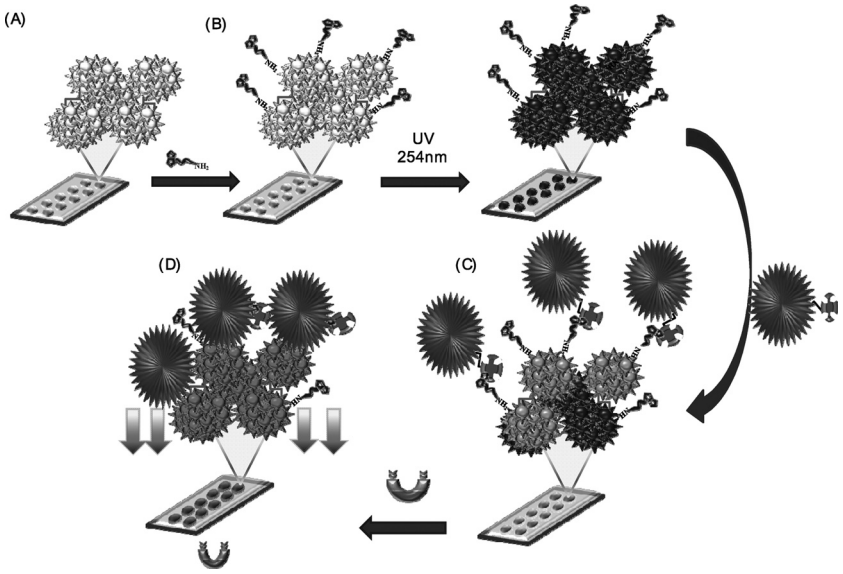

Scheme 1. Schematic representation of biotin-PDA vesicles and their interaction with SA-magnetic beads in colorimetric PDA sensors. A) Preparation of PDA vesicles included 10,12-pentacosadiynoic acid (PCDA) and 1,2-dimyristoyl-sn-glycero- 3-phosphocholine (DMPC) and involved immobilization of PDA vesicles onto the amine-coated glass through *N*-hydroxysuccinimide (NHS)-activated carboxylic acid-amine coupling. Ethylenediamine was then added to cross-link the PDA vesicles. B) After treatment of the liposome surface with NHS/*N*-ethyl-*N*-(3-diethylaminopropyl) carbodiimide hydrochloride (EDC), biotin hydrazine was immobilized onto the PDA vesicles. Next, photopolymerization of the PDA vesicles was carried out using 254 nm UV light. C) Detection of SA-magnetic bead binding. D) Amplification of fluorescent signal using a permanent bar magnet.

bead size. As the size of the magnetic beads became bigger, the fluorescent signal of the PDA vesicle chips increased. Moreover, when a permanent bar magnet was used to cause attraction towards the substrate for enhanced fluorescence, the same relationship between the magnetic bead size and the fluorescence signal strength was observed. The increase in fluorescence from the PDA vesicles with 100 nm magnetic beads was slightly lower than that from PDA vesicles with 1 μm magnetic beads at the same concentration because the extra weight diminished the effects of the mechanical pressure. The changes in fluorescence occurred within about 20 min, which was rapid enough to achieve the desired signal.

The PDA vesicles were conjugated with biotin and their fluorescence signals monitored for SA alone and the SA-conjugated magnetic beads (100 nm and 1μm) in phosphate buffered saline (PBS) buffer (pH 7.4). All experiments were repeated five times and a total of 20 results for each material were obtained. Exact data for each concentration could be obtained based on the average value of the fluorescence signals at each of the four spots.

The PDA vesicles were conjugated with PSA-ACT monoclonal antibody (mAb), and their fluorescent signals were observed in the target PSA-ACT complex solution at concentrations between 0.001 ng mL^{-1} and 10 μg mL^{-1} in PBS buffer (pH 7.4). First, the optimal concentration of PSA-ACT mAb on the PDA vesicle was 5.0 ng mL^{-1} based

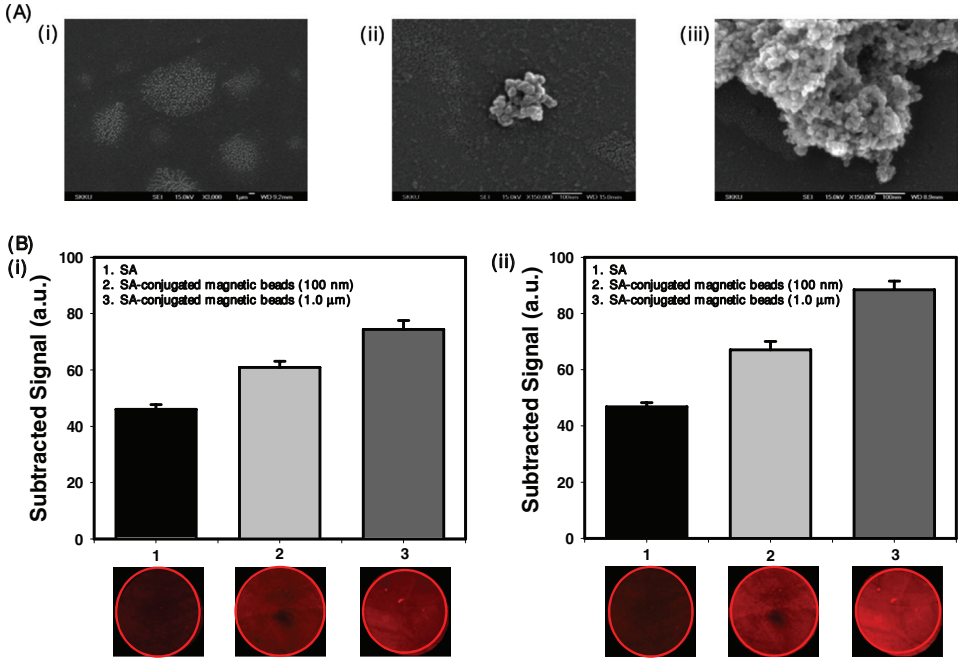

Figure 1. A) SEM image of immobilized PDA spots upon conjugation of the target SA and SA-magnetic beads onto the PDA vesicles following biotin hydrazine immobilization. i) SA; ii) SA-magnetic beads (100 nm); and iii) SA-magnetic beads (1 μm). B) Fluorescence microscopy images and diagram representing the fluorescent signals with i) primary response and ii) enhanced response using a permanent bar magnet after 20 min of attraction at 4 °C.

NANO MICRO small

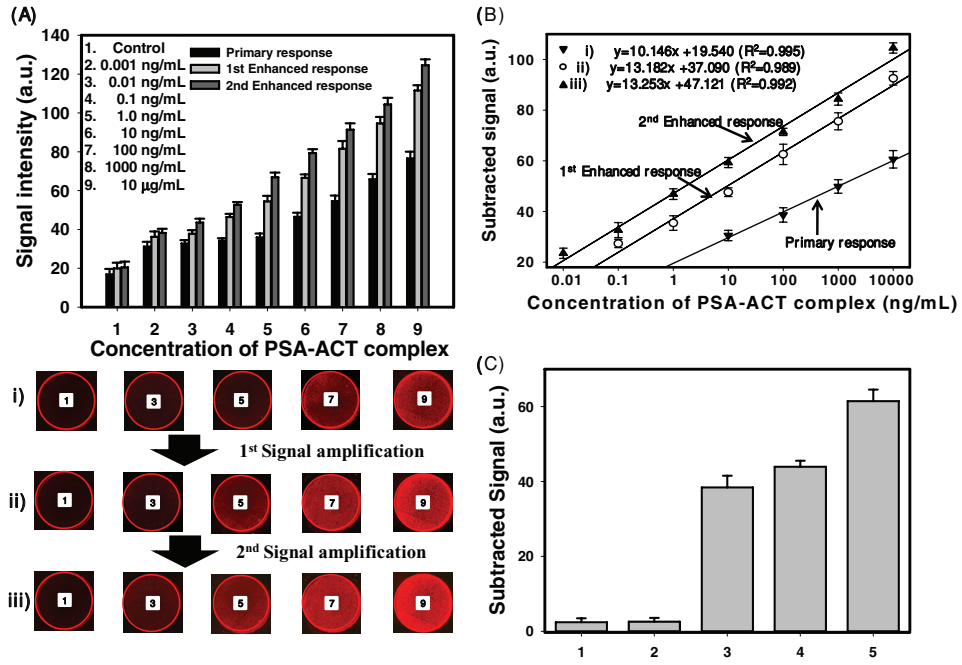

Figure 2. A) Fluorescence microscopy images and diagram representing the fluorescent signals with i) primary response, ii) first enhanced response after 30 min of incubation at 37 °C and iii) second enhanced response using a permanent bar magnet after 20 min of attraction at 4 °C. B) Linear plot of fluorescent responses for the PSA-ACT complex. Three lines indicate: i) primary response, ii) first enhanced response, and iii) second enhanced response of PDA vesicles. C) Non-specific binding of various proteins and PSA pAb-conjugated magnetic beads before and after injection of target PSA-ACT complexes: 1) injection of mixed various proteins (BSA, hIgG, and higE) onto PSA-ACT mAb-conjugated PDA vesicle spots; 2) injection of PSA pAb-conjugated magnetic beads (1μm, 20 μg mL^{-1}) onto PSA-ACT mAb-conjugated PDA vesicle spots; 3) injection of target PSA-ACT complex (100 ng mL^{-1}) onto PSA-ACT mAb-conjugated PDA spots; 4) injection of PSA pAb (20 μg mL^{-1}) after immune reaction with target PSA-ACT complex; and 5) injection of PSA pAb-conjugated magnetic beads (20 μg mL^{-1}) after immune reaction with target PSA-ACT complex. The subtracted signal is the resulting value from the output signal subtracted from the baseline signal derived from reaction with buffer, $n = 5$ (n: number of experiments).

on the fluorescent signal. Detailed results are presented in the Supporting Information. The total quantity of the PSA-ACT complex was estimated by comparing the fluorescent signals of the detection spots with those of the control spots.

The black-colored bars in **Figure 2**A represent the fluorescence intensity and images of the PDA vesicle spots after interaction of the target PSA-ACT complex with PSA-ACT mAb. In this case, the fluorescent signals increased stepwise upon contact with the PSA-ACT complex at concentrations from 10 ng mL^{-1} to 10 μg mL^{-1} in PBS buffer. However, the analytes at concentration below 1 ng mL^{-1} were not determined. The calibration curves for detection of the PSA-ACT complex, which were obtained using the antibody-modified PDA vesicle spots, are shown in Figure 2B. The linear regression equation for detection of the PSA-ACT complex upon interaction with PSA-ACT mAb was: $y = 10.146x + 19.540$ ($R^2 = 0.995$, where R^2 is the coefficient of determination), where y and x are the fluorescence signals of the PDA vesicles and analysis (PSA-ACT complex) concentration (ng mL^{-1}), respectively. However, the PDA vesicle chips in a primary response setting could not be deployed for the detection of PSA cancer markers since biosensors must be sensitive enough to detect concentrations below 4.0 ng mL^{-1}.[19] Therefore, to increase the sensitivity of the PDA vesicle chip, other selective stimuli such as magnetic force are necessary.

To obtain more sensitive detection of the PSA-ACT complex with an antibody-modified PDA vesicle chip, PSA polyclonal antibody (pAb)-conjugated magnetic beads as an external mechanical force for the induction of signal amplification were employed. After the immune response between the PSA-ACT complex and antibody-modified PDA vesicles PSA pAb-conjugated magnetic beads (10 μg mL^{-1} in PBS buffer) were dropped onto the PDA vesicles at 37 °C for the first fluorescent signal enhancement. Here, for the second signal amplification, PSA pAb-conjugated magnetic beads were attracted toward the substrate for 10 min using a permanent bar magnet.

The light grey- and dark grey-colored bars in Figure 2A show the images and fluorescence intensity of the PDA vesicle spots upon application of mechanical force with pAb-conjugated magnetic beads. In this case, the fluorescence signals increased stepwise upon contact with the PSA-ACT complex at concentrations from 0.1 ng mL^{-1} to 10 μg mL^{-1} and from 0.01 ng mL^{-1} to 10 μg mL^{-1}, respectively. However, the analyte was not determined at concentrations below 0.001 ng mL^{-1} (data not shown). The linear regression equation for the enhanced steps was calculated as follows: $y = 13.182x + 37.090$ ($R^2 = 0.989$) and $y = 13.253x + 47.121$ ($R^2 = 0.992$), respectively, as shown in Figure 2B. For the enhanced steps, the linear dynamic range was from 0.01 ng mL^{-1} to

10 μg mL^{-1}, and the detectable minimum concentration was 0.01 ng mL^{-1}. These results show that the sensitivity and dynamic range of the PDA vesicle chips could be effectively improved by mechanical force using pAb-conjugated magnetic beads.

Finally, antibody-modified PDA vesicle chips were analyzed in a mixed solution containing bovine serum albumin (BSA), human immunoglobulin G (hIgG), and human immunoglobulin E (hIgE) to investigate non-specific adsorption. As shown in Figure 2C, bar 1, after the solution was injected onto the PSA-ACT complex mAb-modified PDA vesicle surface, the fluorescence intensities of the various proteins slightly increased. In the absence of any immune reaction between antigen and antibody, the fluorescence intensities in both cases increased negligibly when PSA pAb-conjugated magnetic beads were injected onto the antibody-modified PDA vesicle chips (bar 2). On the other hand, the fluorescence intensities in both cases substantially increased upon immune reaction between the antigen and antibody (bars 3 and 5). Interestingly, the binding of PSA polyclonal antibody (20 μg mL^{-1} in PBS buffer) produced little change in fluorescence intensity (bar 4). The fluorescent signal of the PDA vesicles was already saturated by the antibody–antigen interaction stimulus before introduction of the analyte. These results show that adsorption of the magnetic beads was negligible even at very high concentrations, indicating that an increased mechanical force can be applied as a valuable device along with a low concentration of PDA vesicle chip for applications. We have developed a highly sensitive PDA-based fluorescent microchip to detect a human pathogen. This amplification strategy is widely applicable towards the analysis of other protein biomarkers. Therefore, the presented strategy would open up possibilities for the future use of PDA as a biosensing platform to detect various cancer-associated proteins at ultralow concentrations, both qualitatively and quantitatively.

Experimental Section

Preparation of PDA Vesicles and Immobilization: PCDA and DMPC were separately dissolved in chloroform. Solutions of the two lipid monomers were mixed at a 4:1 molar ratio (PCDA:DMPC) to a total lipid concentration of 1.0 mM. The solvent was removed by purging with N_2 to generate a thin lipid film on the glass surface. The remaining dry film of mixed diacetylene was resuspended in 1.0 mL of 10 mM PBS buffer (pH 7.4) by heating in a circulation water bath at 80 °C with 15 min of gentle stirring. The resulting solution was repeatedly extruded through a prefilter–100 nm membrane–prefilter complex. The extruder system was kept at 90 °C for PCDA and DMPC lipid formation in the dry bath. Then, the vesicle solution was cooled to room temperature (25 °C) over 2 h. Next, NHS and EDC were dissolved separately in PBS buffer to a total concentration of 200 mM. Ethylenediamine (total concentration of 1.0 mM) and the NHS/EDC solution were then added to the vesicle solution. The solutions were arrayed using an automated liquid handling system (Aurora biomed) at room temperature on amine-coated glass. The PDA liposome-arrayed glass was then incubated in a chamber at a constant temperature of 4 °C for 2 h. Interlinking and immobilization of vesicles occurred during incubation, then the PDA liposome-arrayed glass was repeatedly washed with deionized water and 0.1% Tween-20 in water, followed by soft drying under a stream of pure N_2 gas.

Conjugation of PSA-ACT mAb and Detection of PSA-ACT Complex: The PDA vesicles were polymerized by exposure to 254 nm UV light at an intensity of 1.0 mW cm^{-2} for 10 min. NHS/EDC was dissolved in PBS buffer (200 mM) and PSA-ACT mAb was added to the solution. Detection areas were conjugated with the antibody using an automated liquid handling system. After spotting the antibody, the PDA vesicle-arrayed glass was incubated in a constant temperature chamber at 4 °C for 3 h, followed by gentle washing with deionized water and drying under pure N_2 gas. The PSA-ACT complex was then dropped on the antibody-conjugated PDA vesicles, followed by incubation at 37 °C for 30 min. PBS buffer was added to the PDA vesicle conjugate as a baseline. After 30 min, the change in fluorescence was analyzed by fluorescence microscopy.

Signal Amplification Using PSA pAb-Conjugated Magnetic Beads: First, biotinylation of PSA-ACT mAb, purification of the biotinylated mAb, and measurement of the level of biotin incorporation were carried out using an EZ-link sulfo-NHS-LC-Biotinylation Kit according to the manufacturer's protocol. Then, biotinylated PSA pAb (20 μg mL^{-1} in PBS buffer pH 7.4) was added to the SA-conjugated magnetic beads (1.0 μg mL^{-1}) at 0.5 mL, followed by incubation at room temperature for 3 h. The PSA pAb-conjugated magnetic beads were centrifuged at 15 000 × g for 45 min at 4 °C to remove excess PSA pAb. The conjugated magnetic beads were then resuspended in 5.0 mL of 0.01 M PBS buffer (pH 7.4) and stored at 4 °C.

Amplification of the PDA vesicle signal was confirmed using a sandwich immunoassay based on the attraction of magnetic beads. After the immune response between the PSA-ACT complex and mAb, PSA pAb-conjugated magnetic beads (10 μg mL^{-1} in PBS buffer) were dropped onto the PDA vesicles, conjugated, and incubated for 30 min at 37 °C for the first enhancement step. After incubation, the change in fluorescence was analyzed by fluorescence microscopy. After analysis, PSA pAb-conjugated magnetic beads were attracted towards the substrate at 4 °C for 20 min using a permanent bar magnet for the second enhancement step. Again, any change in fluorescence was analyzed by fluorescence microscopy.

Supporting Information

Supporting Information is available from the Wiley Online Library or from the author.

Acknowledgements

This work was supported by the Korea Science and Engineering Foundation (KOSEF) National Research Laboratory (NRL) Program (R0A-2008-000-20078-0), Basic Science Research Program (2010-0027771), and grant (DG2-201) from Carbon Dioxide Reduction & Sequestration Research Center, one of the 21st Century Frontier Programs funded by the Ministry of Science and Technology of Korean government of the Republic of Korea.

[1] I. B. Kim, U. H. F. Bunz, *J. Am. Chem. Soc.* **2006**, *125*, 2818.
[2] S. Kolusheva, T. Shahal, R. Jelinek, *J. Am. Chem. Soc.* **2000**, *122*, 776.
[3] J. S. Yang, T. M. Swager, *J. Am. Chem. Soc.* **1998**, *120*, 5321.
[4] D. J. Ahn, E. H. Chae, G. S. Lee, H. Y. Shim, T. E. Chang, K. D. Ahn, J. M. Kim, *J. Am. Chem. Soc.* **2003**, *125*, 8976.
[5] Q. Cheng, R. C. Stevens, *Langmuir* **1998**, *14*, 1974.
[6] S. W. Lee, C. D. Kang, D. H. Yang, J. S. Lee, J. M. Kim, D. J. Ahn, S. J. Sim, *Adv. Funct. Mater.* **2007**, *17*, 2038.
[7] N. Mino, H. Tamura, K. Ogawa, *Langmuir* **1992**, *8*, 597.
[8] R. A. Nallicheri, M. F. Rubner, *Macromolecules* **1991**, *24*, 517.
[9] H. Ringsdorf, B. Schlarb, J. Venzmer, *Angew. Chem. Int. Ed.* **1988**, *27*, 113.
[10] D. J. Ahn, S. M. Lee, J. M. Kim, *Adv. Funct. Mater.* **2008**, *18*, 1.
[11] C. H. Park, J. P. Kim, S. W. Lee, N. L. Jeon, P. J. Yoo, S. J. Sim, *Adv. Funct. Mater.* **2009**, *19*, 3703.
[12] Y. K. Jung, T. W. Kim, C. Jung, D. Y. Cho, H. G. Park, *Small* **2008**, *4*, 1778.
[13] S. Loeb, W. J. Catalona, *Cancer Lett.* **2007**, *249*, 30.
[14] Z. Ma, J. Li, J. Cao, Z. Zou, J. Tu, L. Jiang, *J. Am. Chem. Soc.* **1998**, *120*, 12678.
[15] D. Seo, J. Kim, *Adv. Funct. Mater.* **2010**, *20*, 1397.
[16] I. K. Kwon, J. P. Kim, S. J. Sim, *Biosens. Bioelectron.* **2010**, *26*, 1548.
[17] T. T. H. Pham, S. J. Sim, *J. Nanopart. Res.* **2010**, *12*, 227.
[18] C. Cao, X. Li, J. Lee, S. J. Sim, *Biosens. Bioelectron.* **2009**, *24*, 1292.
[19] D. A. Healy, C. J. Hayes, P. Leonard, L. McKenna, R. O'Kennedy, *Trends Biotechnol.* **2007**, *25*, 125.

Received: July 2, 2011
Published online: November 15, 2011